J Fluoresc (2011) 21:161–167
DOI 10.1007/s10895-010-0700-7

ORIGINAL PAPER

Development of Fluorescent Array Based on Sol-Gel/ Chitosan Encapsulated Acetylcholinesterase and pH Sensitive Oxazol-5-one Derivative

Gulsiye Ozturk · Karl-Heinz Feller · Kay Dornbusch · Suna Timur · Serap Alp · Yavuz Ergun

Received: 9 April 2010 / Accepted: 22 June 2010 / Published online: 9 July 2010

Abstract A highly sensitive fluorescent enzyme array for quantitative acetylcholine detection is developed. The enzyme array has been constructed by spotting of pH sensitive fluorophore 2-phenyl-4-[4-(1,4,7,10-tetraoxa-13-azacycloopentadecyl)benzylidene]oxazol-5-one and acetylcholinesterase doped in tetraethoxysilane / chitosan matrix via a microarrayer. The constructed tetraethoxysilane / chitosan network provided a microenvironment in which the enzyme molecule was active biologically. The optimal operational conditions for the array developed were investigated. The response of the developed biosensor array to acetylcholine was highly reproducible (RSD=3.27%, n= 6). A good linearity was observed for acetylcholine in the concentrations up to 1×10^{-8} M, with a detection limit of 0.27×10^{-8} M.

Keywords Fluorescent array · Sol-gel · Chitosan · Acetylcholinesterase · Acetylcholine · Biosensor

G. Ozturk · S. Alp · Y. Ergun
Faculty of Arts and Sciences,
Department of Chemistry, University of Dokuz Eylul,
Tinaztepe,
35160 Izmir, Turkey

G. Ozturk (✉) · K.-H. Feller · K. Dornbusch
Department of Medical Engineering and Biotechnology,
University of Applied Sciences Jena,
Carl-Zeiss-Promenade 2,
07745 Jena, Germany
e-mail: gulsiye.ozturk@deu.edu.tr

S. Timur
Faculty of Science, Department of Biochemistry, Ege University,
Bornova,
35100 Izmir, Turkey

Introduction

The development of new biosensing systems and biosensor arrays is currently the subject of extensive research in areas such as clinical diagnostic, food technology, biomedical and environmental analysis [1–15]. Miniaturization is currently a very important aspect in biosensing technology because of its effectiveness in reducing cost, labor, and allowing for rapid analysis [2, 16, 17]. This aspect of miniaturization is well matched with the ultimate goal of rapid screening. The importance of enzyme-based biosensors has increased considerably in the last years thanks to exceptional properties which include high specificity, rapid response and low cost. One of the most important steps in the development of these kinds of biosensors is the immobilization of the enzymatic system in an appropriate solid support which integrates the bio molecules maintaining their functionality, allowing performing reactions in a sequential order while providing accessibility towards the target analyte and subsequent substrates. The sensing of a chemical environment is achieved mainly in the surface interactions of the sensor material with its chemical surroundings. Therefore, a porous structure is of great importance in developing good chemical sensors [5, 14]. Compared to other immobilization methods, such as adsorption to solid supports, covalent attachment and polymer entrapment, the sol-gel chemistry show numerous advantages including entrapment of large amount of enzymes, thermal and chemical stability of the matrix, enhanced stability of the encapsulated biomolecules, excellent optical transparency and flexibility in controlling the pore size and geometry. Furthermore, the porous nature of the matrix, retains the natural conformation and the reactivity of enzymes and had positive influence on enzyme activity and production of desired products due to its

specific interactions with the biomaterial and the reaction mixture [6, 8–10].

In recent years, the use of acetylcholinesterase (AChE) in biosensor technology has gained enormous attention, in respect to pesticide and drug detection [8–11, 14, 15]. The determination of choline esters and particularly acetylcholine (ACh) is of interest for clinical and analytical purposes [15]. ACh plays an important role as neurotransmitter both in the central nervous system and in the nerve skeletal junction. The detection of ACh by fluorimetric method is based on the inhibition of AChE. After the hydrolysis of acetylcholine by AChE, acetic acid and choline will be produced, thereby decreasing the pH value and causing a fluorescence change if there is a pH-sensitive fluorescent indicator system. There are many methods for pH measurement at present. However, fluorescence offers significant advantages over other methods for physiological pH measurements due to its generally non-destructive character, high sensitivity and specificity, and the wide range of indicator dyes available [18–20]. Fluorescent pH indicators that can sense pH changes within the physiological range are an attractive target in molecular design and synthesis.

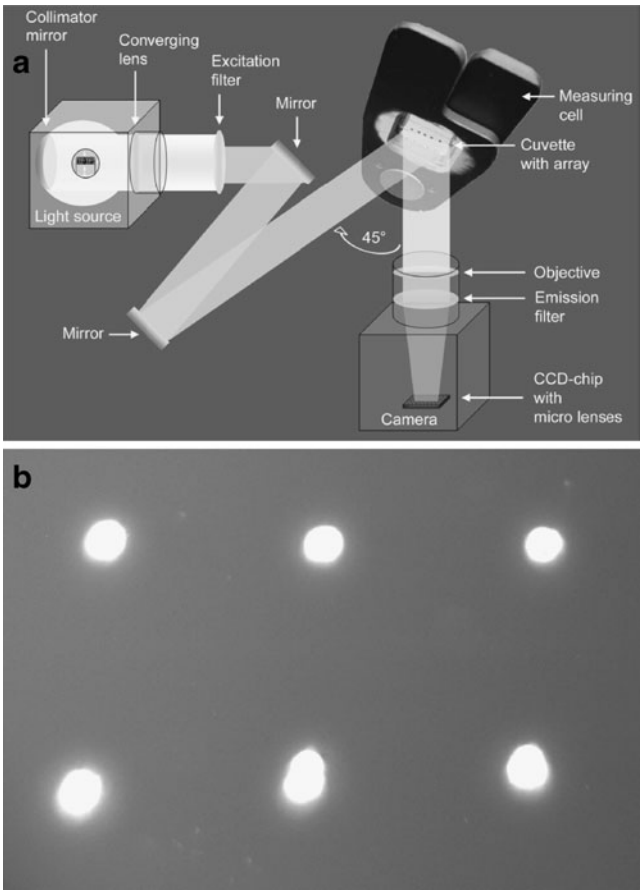

Fig. 1 **a** Scheme of the fluorescence measuring set-up [31]. **b** Fluorescence image of TEOS/CHIT/CPO/AChE spots

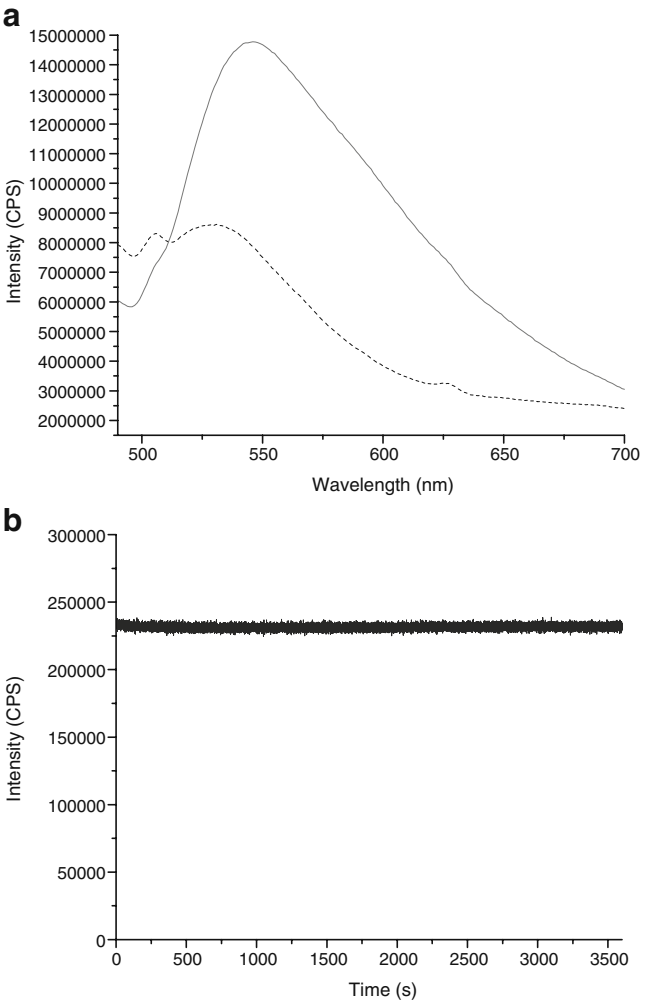

Fig. 2 **a** The fluorescence spectra of TEOS/CHIT/CPO/AChE array (—) in plain buffer of 5 mM pH 7 phosphate buffer and (—) 10^{-5} M ACh containing 5 mM pH 7 phosphate buffer. **b** Photo stability result of CPO in TEOS/CHIT matrix

Edrophonium chloride (EC) is a very short-acting AChE inhibitor administered by the intravenous or intramuscular routes [21, 22]. It is primarily used in diagnostic tests for the confirmation of myasthenia gravis, and differentiating between the presences of a myasthenic or cholinergic crisis. It can be used in combination with atropine when patients do not breathe spontaneously postoperatively after the application of competitive neuromuscular blocking drugs such as atracurium. It acts indiscriminately at muscarinic and nicotinic receptor sites.

Pyridostigmine bromide (PB) is a quaternary dimethyl carbamate that reversibly inhibits acetylcholinesterase (AChE) in the peripheral nervous system, thus limiting irreversible inhibition of the enzyme by nerve agents [23–27]. AChE activity is restored following spontaneous decarbamylation resulting in near-normal neuromuscular and autonomic functions.

In our previous study, we immobilized AChE and different oxazol-5-one derivatives in polyvinylchloride (PVC) matrix [28, 29]. The present study, which is an extension of our early studies [28, 29] reports the development of a new biosensing array based on tetraethoxysilane (TEOS) / Chitosan (CHIT) matrix with fluorescence measuring set-up system for detection of acetylcholine as well as AChE inhibitors. A pH sensitive fluorescent derivative 2-phenyl-4-[4-(1,4,7,10-tetraoxa-13-azacycloopentadecyl)benzylidene]oxazol-5-one (CPO) was mixed in TEOS/CHIT together with the enzyme and spotted onto microscope slides by using a microarrayer. In order to measure the response of the arrays, the pH induced changes in fluorescence intensity of the dye due to the enzymatic reaction were followed. In this system, the sensitivity is improved approximately 1000 fold in comparison to the previous ones [28, 29]. The inhibition efficiencies of EC and PB on activity of immobilized AChE were also evaluated.

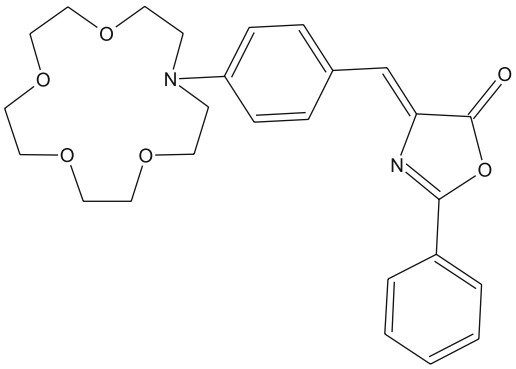

CPO

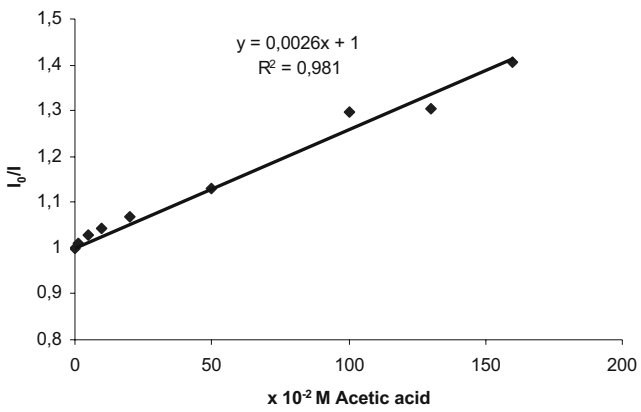

Fig. 3 Stern-Volmer plot of 10^{-5} M CPO in THF quenched by acetic acid

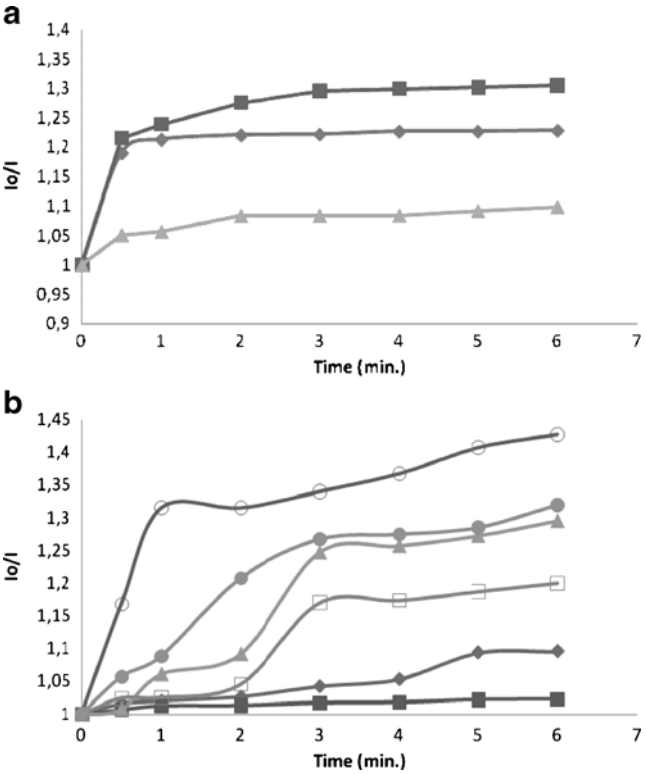

Fig. 4 **a** Effect of pH on the response of TEOS/CHIT/CPO/AChE array at pH (■) 7.0; (♦) 6.0 and (▲) 8.0; Io refers to the fluorescence intensity obtained at plain phosphate buffer and I to the fluorescence intensity obtained at 10^{-6} M ACh at 30 mM pH 7.0 phosphate buffer. **b** Ionic strength effect on the response of TEOS/CHIT/CPO/AChE array (○) 5, (●) 1, (▲) 10, (□) 2.5, (♦) 50 and (■) 20 mM pH 7 phosphate buffer; Io refers to the fluorescence intensity obtained at plain pH 7 phosphate buffer and I to the fluorescence intensity obtained at 4×10^{-7} M ACh containing pH 7 phosphate buffer

Experimental

Reagents

The synthesis and purification of fluorescent CPO derivative used in the detection of ACh has been reported earlier [30]. Acetylcholinesterase (AChE; EC 3.1.1.7, from Electric EL, 500 U mg^{-1}), acetylcholine chloride, glutaraldehyde, tetraethylorthosilicate (TEOS), edrophonium chloride and pyridostigmine bromide were purchased from Sigma (Germany). KH_2PO_4 was obtained from Riedel-de Haen® (Germany).

Construction of TEOS/CHIT/CPO/AChE array

Sol-gel/chitosan solution was prepared by mixing different amounts of TEOS and ethanol with 600 μL of 0.5 $mg ml^{-1}$ chitosan solution. This mixture was stirred for 1 h until a clear sol-gel composite was formed and its pH was adjusted 4.0–6.0 by using 0.1 M NaOH solution [9, 10].

The TEOS/CHIT/CPO/AChE array is generated by mixing 100 μL sol-gel/chitosan solution, 50 μL of 50 U ml^{-1} AChE

and 70 μL of 1 mgml^{-1} CPO derivative and spotting this solution on cleaned microscope slides. After drying, spots were treated with glutaraldehyde solution (2.5% in potassium phosphate buffer, 50 mM, pH 7.0) for 2 min and washed with distilled water and phosphate buffer solution, respectively.

Apparatus and the detection system setup

BioRobotics MicroGrid, A High Throughput Automated Microarrayer (England) was used for spotting of sol-gel/chitosan solution on the surface of the glass slides. For the fluorescent intensity measurement of the spots, Sensovation AG, Stockach (Germany) control system (Fig. 1a) was used [31]. Absorption measurements were performed with a UV–Vis spectrophotometer (Perkin Elmer- UV/VIS Spectrometer-Lambda 2, (Germany)). Fluorescence spectral data were recorded on Horiba JOBIN YVON Fluoromax-4 Spectrofluorometer (Germany). The pH values of buffer solutions were adjusted with VWR digital pH-meter (Germany) calibrated with Merck pH standards of pH 7.00 and pH 4.01.

The measuring arrangement– a fluorescence reader (Sensovation AG, Stockach) (Fig. 1a)—consists of a lamp, a shutter, filters for excitation and emission and a 3-stage Peltier cooled CCD image sensor with integrated micro-lenses and a high quantum efficiency (up to 90%) for detecting the fluorescence signal.

The chip array is located in front of the fluorescence camera which is gathering as much fluorescence light as possible. The excitation light, passing the filters for wavelength selection, is directed onto the front of the measuring cell via mirrors. Additional filters in front of the camera enable a reduction of the stray light and a pre-selection of the detection wavelength region [31]. The excitation light can be also directed to the backside of the cell for adsorption measurements. Such a modular set-up made the measuring console very flexible to various measuring regimes. The emitted radiation is taken by a deep cooled CCD camera.

The image detected by means of the digital camera (Fig. 1b) consists of data regions from the spotted area together with a huge background region around. Technological spotting of the indicator volume onto the slide does not yield a uniform centred spotting but the spots jitter around the centre position. To reduce the background signal contributing to the averaged signal intensity taken from the spotted area, a spot recognition software module (Iconoclust, Clondiag GmbH Jena) was used to accumulate the signals in the spotted area only.

Measuring procedure

The TEOS/CHIT/CPO/AChE arrays were subjected to plain phosphate buffer solutions and buffer solutions

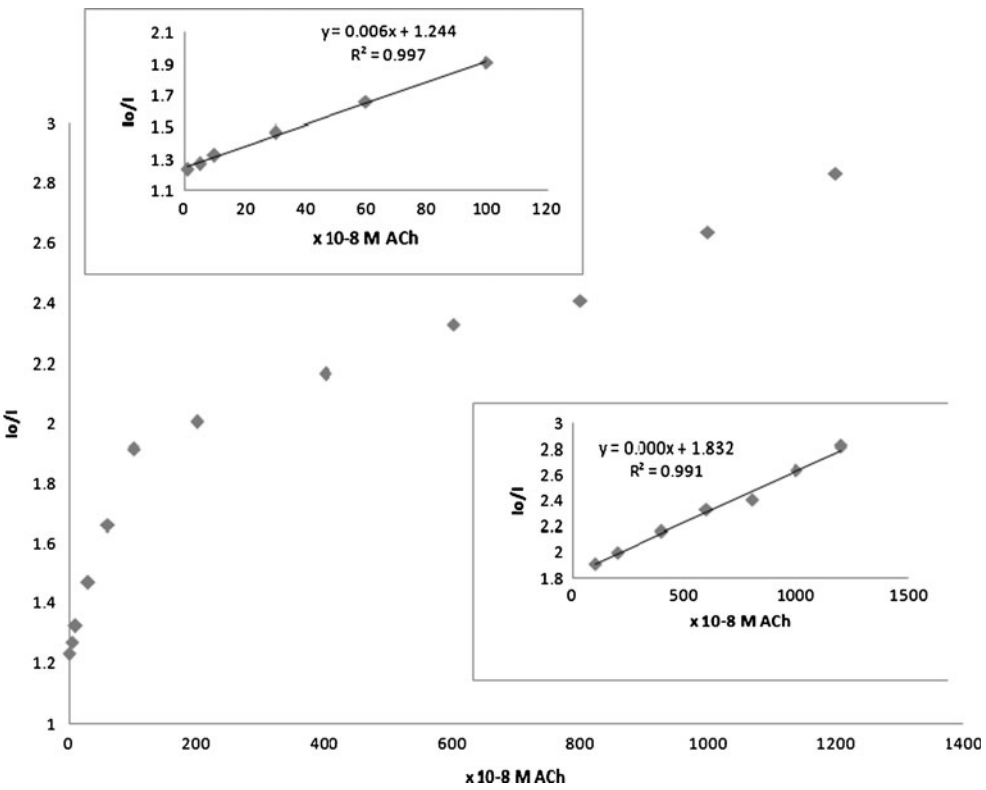

Fig. 5 Response of the TEOS/CHIT/CPO/AChE array in the concentration range of 1×10^{-8} to 1.2×10^{-6} M ACh

containing different concentrations of ACh for 3 min and emissions were collected at 540 nm under 460 nm excitation wavelength. AChE catalyzes the hydrolysis of acetylcholine into choline and acetic acid, as shown below (Eq. 1):

$$\text{Acetylcholine} + H_2O \xrightarrow{\text{AChe}} \text{Acetic acid} + \text{Choline} \quad (1)$$

The acid dissociates further to release H^+ ions, which cause decrease of fluorescence intensity of CPO.

Results and discussion

The fluorescence behaviour of CPO in TEOS/CHIT

Figure 2a depicts the emission spectra of CPO in the absence (—curve) and presence (— curve) of ACh at 5 mM pH 7 phosphate buffer. The excitation and emission peaks of CPO in sol-gel / chitosan matrix at plain 5 mM pH 7 phosphate buffer, were observed at 460 and 545 nm respectively. After exposure to 10^{-5} M ACh containing 5 mM pH 7 phosphate buffer the fluorescence intensity of CPO was quenched and blue shift of the emission of 15 nm leading to a fluorescence maximum of 530 nm was observed as shown in Fig. 2a.

The photostability test of CPO dye in TEOS/CHIT matrix was performed with a steady state spectrofluorimeter in mode of time-based measurements. The data in Fig. 2b, acquired at 545 nm emission after 1 h of monitoring, reveals the excellent photo stability of CPO in TEOS/CHIT matrix.

The fluorescence images of TEOS/CHIT/CPO/AChE spots were obtained by collecting the emission intensity at 540 nm under 460 nm excitation wavelengths with the measuring arrangement– a fluorescence reader (Sensovation AG, Stockach) shown in Fig. 1a (Fig. 1b).

Statistic and dynamic quenching rate constants

In the case of energy quenching by encounter complexes, the dynamical quenching, the fluorescence lifetime follows the Stern-Volmer relation [32] (Eq. 2):

$$I_0/I = 1 + \tau_F k_q [Q] \quad (2)$$

where I_0 is the initial fluorescence intensity and I is the fluorescence intensity in the presence of quencher, τ_F fluorescence lifetime, k_q rate constant and [Q] the quencher concentration. Diffusion-controlled (or diffusion-limited) reactions are reactions that occur so quickly that the reaction rate is the rate of transport of the reactants through the reaction medium (usually a solution). In this case the quenching rate constant is mainly determined by the diffusion rate constant.

The Stern-Volmer plots of the fluorescence quenching experiments of CPO in a TEOS/CHIT matrix show in all cases a non-linear dependence with two ascents, indicating two different quenching processes. From the system it is obviously that the quenching can be due to static and dynamic quenching as well. To calculate the two different quenching rate constants from the Stern-Volmer plot at first the fluorescence lifetime must be known. For this reason quenching experiments of a 10^{-5} M CPO solution in THF by acetic acid were made. The received Stern-Volmer plots show (as depicted in Fig. 3) the expected straight line dependence. From the ascent of the curve the fluorescence lifetime of CPO was estimated to 12.5 ps. Using this fluorescence lifetime, the rate constants of the two processes found in the Stern-Volmer plots of the matrix system (TEOS/CHIT) can be calculated to 5.4×10^8 s^{-1}

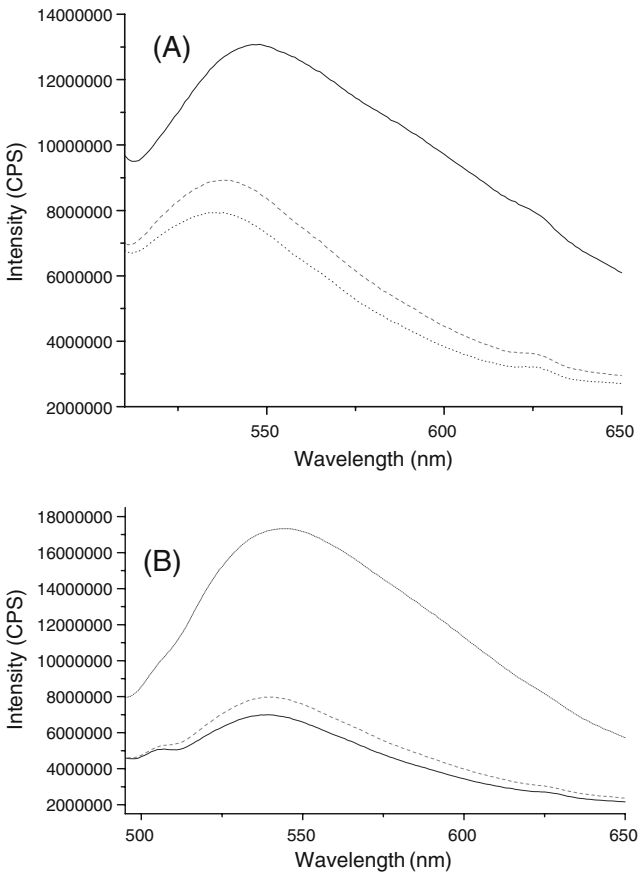

Fig. 6 **a** Emission spectra of the TEOS/CHIT/CPO/AChE array in (—) plain 5 mM pH7 phosphate buffer, (—) 10^{-5} M ACh containing 5 mM pH 7 phosphate buffer and (···) 10^{-5} M ACh and 10^{-4} M EC containing 5 mM pH 7 phosphate buffer. **b** Emission spectra of the TEOS/CHIT/CPO/AChE array in (·—·—) plain 5 mM pH7 phosphate buffer, (—) 10^{-5} M ACh containing 5 mM pH 7 phosphate buffer and (—) 10^{-5} M ACh and 10^{-4} MPB containing 5 mM pH 7 phosphate buffer

(static quenching rate constant) and 6.7×10^{7} s^{-1} (dynamic quenching rate constant), respectively for CPO in TEOS/CHIT/CPO/AChE array.

Effect of pH and ionic strength on response of TEOS/CHIT/CPO/AChE array

The effect of pH on the response was tested at pH 6.0, 7.0 and 8.0 (Fig. 4a). The optimum response of the TEOS/CHIT/CPO/AChE array was obtained at pH 7.0. This result indicates that TEOS/CHIT matrix did not alter the optimal pH value for catalytic behaviour of enzyme and the microenvironment surrounding the enzyme in the sol-gel pores was easily accessed by substrate. In order to avoid the other interfering pH dependent signal fluctuations, all the measurements were performed at pH 7.0 phosphate buffer. In Fig. 4a, it is clearly observed that the fluorescence intensity achieved its maximum at 3 min. Therefore, we used this response time in our further experimental steps.

To increase the TEOS/CHIT/CPO/AChE array's response, the effect of ionic strength was also investigated. For this purpose, phosphate buffer solutions (pH 7.0) with different ionic strength (1, 2.5, 5, 10, 25 and 50 mM) were prepared and fluorescence intensities of TEOS/CHIT/CPO/AChE array in the presence of 4×10^{-7} M ACh in the prepared buffer solutions were measured (Fig. 4b). The highest response was obtained with 5 mM and it was chosen as the most appropriate measurement medium.

Analytical characteristics of the TEOS/CHIT/CPO/AChE array system

Figure 5, shows the response of the TEOS/CHIT/CPO/AChE array in the concentration range of 1×10^{-8} to 1.2×10^{-6} M ACh and the linearity was observed at two concentration ranges of 1×10^{-8}–1×10^{-6} and 1×10^{-6}–1.2×10^{-5} M ACh.

The limit of detection (LOD) for ACh was defined as the concentration at which the signal is equal to the average blank signal ±3 standard deviation (n=5). LOD value for ACh was calculated as 0.27×10^{-8} M.

The repeatability of the TEOS/CHIT/CPO/AChE arrays was tested for 30×10^{-7} M ACh by 6 successive measurements and the relative standard deviation (RSD) was calculated as 3.27%.

Inhibition effect of different drugs on activity of immobilized AChE

Pure medicines of EC and PB were selected to evaluate their inhibition efficiencies on activity of immobilized AChE. As shown from Fig. 6a and b, after sensor array was immersed in 10^{-4} M EC and PB containing 5 mM pH 7 phosphate buffer solutions of two medicines, the emission intensities of CPO decreased 11% and 12%, respectively in comparison to the fluorescence intensity observed at ACh containing 5 mM pH 7 phosphate buffer.

In our previous study where we immobilized AChE and different oxazol-5-one derivatives in polyvinylchloride (PVC) matrix [28, 29] which is also solid matrix like TEOS/CHIT, the sensor stability was tested and the results obtained indicate that the stability of the sensor system is satisfactory in solid matrix.

Conclusion

The results presented here report the development of optical TEOS/CHIT/CPO/AChE array for the detection of acetylcholine using the fluorescence intensity decrease of CPO. The large quantities of hydroxyl groups in the sol-gel hybrid material formed strong hydrogen bonds, which interacted with the immobilized enzyme and prevented them from leaking out of the film, thus AChE has been successfully immobilized. The array exhibited good sensitivity towards acetylcholine, with a linear response in the concentration ranges of 1×10^{-8}–1×10^{-6} and 1×10^{-6}–1.2×10^{-5} M. The response of the biosensor array to ACh was highly reproducible (RSD=3.27%).

To sum up, the developed optical TEOS/CHIT/CPO/AChE array is a simple, sensitive, accurate and low-cost technique. These characteristics are very attractive for the possible miniaturization. In our further studies we aim to incorporate the developed TEOS/CHIT/CPO/ACh array into a microfluidic technology, thus to provide a micro-sensor system.

References

1. Luong JHT, Male KB, Glennon JD (2008) Biosensor technology: technology push versus market pull. Biotechnol Adv 26:492–500
2. Maloney JM, Uhland SA, Polito BF, Sheppard NF, Pelta CM, Santini JT (2005) Electrothermally activated microchips for implantable drug delivery and biosensing. J Control Release 109:244–55
3. Ramanathan M, Simonian AL (2007) Array biosensor based on enzyme kinetics monitoring by fluorescence spectroscopy: application for neurotoxins detection. Biosens Bioelectron 22:3001–7
4. Tsai H, Doong R (2005) Simultaneous determination of pH, urea, acetylcholine and heavy metals using array-based enzymatic optical biosensor. Biosens Bioelectron 20:1796–804
5. Xi Y, Liangying Z, Sasa W (1995) Pore size distribution control of porous silica. Sens Actuators, B, Chem 25:347–52
6. Kuncova G, Podrazky O, Ripp S, Trögl J, Sayler GS, Demnerova K, Vankova R (2004) Monitoring of the viability of cells immobilized by sol-gel process. J Sol-Gel Sci Technol 31:335–42
7. Salinas-Castillo A, Pastor I, Mallavia R, Mateo CR (2008) Immobilization of a trienzymatic system in a sol-gel matrix: a

new fluorescent biosensor for xanthine. Biosens Bioelectron 24:1053–6
8. Anitha K, Mohan SV, Reddy SJ (2004) Development of acetylcholinesterase silica sol-gel immobilized biosensor-an application towards oxydemeton methyl detection. Biosens Bioelectron 20:848–56
9. Du D, Chen S, Cai J, Song D (2007) Comparison of drug sensitivity using acetylcholinesterase biosensor based on nanoparticles-chitosan sol-gel composite. J Electroanal Chem 611:60–6
10. Du D, Chen S, Cai J, Zhang A (2007) Immobilization of acetylcholinesterase on gold nanoparticles embedded in sol-gel film for amperometric detection of organophosphorus insecticide. Biosens Bioelectron 23:130–4
11. Du D, Chen S, Cai J, Zhang A (2008) Electrochemical pesticide sensitivity test using acetylcholinesterase biosensor based on colloidal gold nanoparticle modified sol-gel interface. Talanta 74:776–82
12. Paliwal S, Wales M, Good T, Grimsley J, Wild J, Simonian A (2007) Fluorescence-based sensing of p-nitrophenol and p-nitrophenyl substituent organophosphates. Anal Chim Acta 596:9–15
13. Dan D, Shizhen C, Jie C, Aidong Z (2007) Immobilization of acetylcholinesterase on gold nanoparticles embedded in sol-gel film for amperometric detection of organophosphorus insecticide. Biosens Bioelectron 23:130–4
14. Doong RA, Tsai HC (2001) Immobilization and characterization of sol-gel-encapsulated acetylcholinesterase fiber-optic biosensor. Anal Chim Acta 434:239–46
15. Doretti L, Ferrara D, Lora S, Schiavon F, Veronese FM (2000) Acetylcholine biosensor involving entrapment of acetylcholinesterase and poly(ethylene glycol)-modified choline oxidase in a poly(vinyl alcohol) cryogel membrane. Enzyme Microb Technol 27:279–85
16. Song JM, Griffin GD, Vo-Dinh T (2003) Application of an integrated microchip system with capillary array electrophoresis to optimization of enzymatic reactions. Anal Chim Acta 487:75–82
17. Drill K, Montgomery DD, Wang W, Tsai JC (2001) Antigen detection using microelectrode array microchips. Anal Chim Acta 444:69–78
18. Haugland RP (2002) Handbook of fluorescent probes and research products. Molecular Probes, Eugene
19. Haugland RP (2005) The handbook. a guide to fluorescent probes and labeling technologies, 10th ed. Molecular Probes, Inc., Eugene, pp 935–947
20. Qin W, Baruah M, De Borggraeve WM, Boens N (2006) Photophysical properties of an on/off fluorescent pH indicator excitable with visible light based on a borondipyrromethene-linked phenol. J Photochem Photobiol, A Chem 183:190–7
21. Corea N (2007) Edrophonium. Elsevier, Bedford, p 1
22. Luo C, Saxena A, Ashani Y, Leader H, Radic Z, Taylor P, Doctor BP (1999) Role of edrophonium in prevention of the re-inhibition of acetylcholinesterase by phosphorylated oxime. Chem-Biol Interact 119–120:129–35
23. Abou-Donia MB, Dechkovskaia AM, Goldstein LB, Abdel-Rahman A, Bullman SL, Khan WA (2004) Co-exposure to pyridostigmine bromide, DEET, and/or permethrin causes sensorimotor deficit and alterations in brain acetylcholinesterase activity. Pharmacol Biochem Behav 77:253–62
24. Gordon RK, Haigh JR, Garcia GE, Feaster SR, Riel MA, Lenz DE, Aisen PS, Doctor BP (2005) Oral administration of pyridostigmine bromide and hyperzine A protects human whole blood cholinesterases from ex vivo exposure to soman. Chem-Biol Interact 157–158:239–46
25. Kant GJ, Bauman RA, Feaster SR, Anderson SM, Saviolakis GA, Garcia GE (2001) The combined effects of pyridostigmine and chronic stress on brain cortical and blood acetylcholinesterase, corticosterone, prolactin and alternation performance in rats. Pharmacol Biochem Behav 70:209–18
26. Servatius RJ, Ottenweller JE, Guo W, Beldowicz D, Zhu G, Natelson BH (2000) Effects of inescapable stress and treatment with pyridostigmine bromide on plasma butyrylcholinesterase and the acoustic startle response in rats. Physiol Behav 69:239–46
27. Sinton CM, Fitch TE, Petty F, Haley RW (2000) Stressful manipulations that elevate corticosterone reduce blood-brain barrier permeability to pyridostigmine in the rat. Toxicol Appl Pharmacol 165:99–105
28. Ozturk G, Alp S, Timur S (2007) A fluorescent biosensor based on acetylcholinesterase and 5-oxazolone derivative immobilized in polyvinylchloride (PVC) matrix. J Mol Catal B Enzym 47:111–6
29. Ozturk G, Alp S, Timur S (2008) Photophysical characterization of fluorescent oxazol-5-one derivatives in PVC and their application as biosensors in the detection of ACh and AChE inhibitor: Donepezil. Dyes Pigm 76:792–89
30. Öztürk G, Alp S, Ergün Y (2007) Synthesis and Spectroscopic properties of new 5-oxazolone derivatives containing an N-phenyl-aza-15-crown-5 moiety. Tetrahedron Lett 48:7347–50
31. Schimmelpfennig M, Dornbusch K, Bannert M, Feller KH (2008) Micro-structured devices for chemical sensing of flavor and fragrance. Eng Life Sci 8:415–24
32. Brückner V, Feller KH, Grummt UW (1990) Application of time-resolved optical spectroscopy. Elsevier Science, Amsterdam, p 120